

Published in final edited form as:

*Neuron*. 2008 August 14; 59(3): 475–485. doi:10.1016/j.neuron.2008.07.006.

## Local dendritic activity sets release probability at hippocampal synapses

Tiago Branco<sup>1,2,\*</sup>, Kevin Staras<sup>1,3</sup>, Kevin J. Darcy<sup>1</sup>, and Yukiko Goda<sup>1,2,\*</sup>

<sup>1</sup>MRC Laboratory for Molecular Cell Biology and Cell Biology Unit, University College London, Gower Street, London WC1E 6BT, UK

<sup>2</sup>Department of Neuroscience, Physiology & Pharmacology, University College London, Gower Street, London WC1E 6BT, UK

<sup>3</sup>School of Life Sciences, University of Sussex, Brighton, BN1 9QG, UK

### Abstract

The arrival of an action potential at a synapse triggers neurotransmitter release with a limited probability,  $p_r$ . Although  $p_r$  is a fundamental parameter in defining synaptic efficacy, it is not uniform across all synapses and the mechanisms by which a given synapse sets its basal release probability are unknown. By measuring  $p_r$  at single presynaptic terminals in connected pairs of hippocampal neurons, we show that neighboring synapses on the same dendritic branch have very similar release probabilities, and  $p_r$  is negatively correlated with the number of synapses on the branch. Increasing dendritic depolarization elicits a homeostatic decrease in  $p_r$ , and equalizing activity in the dendrite significantly reduces its variability. Our results indicate that local dendritic activity is the major determinant of basal release probability, and we suggest that this feedback regulation might be required to maintain synapses in their operational range.

### Introduction

Release probability ( $p_r$ ) is the likelihood of vesicle fusion and transmitter release occurring at a presynaptic terminal in response to an action potential (Del Castillo and Katz, 1954). This fundamental parameter is critical in determining the strength of a synapse as well as its dynamic adaptation to input and, as such, it shapes the nature of neuron-neuron communication (Maass and Zador, 1999). Studies from a variety of systems indicate that release probability at individual synapses is unique (Atwood and Bittner, 1971; Frank, 1973; Cooper et al, 1996; Dobrunz and Stevens, 1997). However, the factors contributing to the setting of  $p_r$  at each synaptic terminal still remain to be determined. Extensive experimental evidence, from work on neuromuscular junction and invertebrate and vertebrate central synapses, has suggested that the setting of release probability along single axons can be related to the identity of the postsynaptic target (Bennett et al, 1986; Robitaille and Tremblay, 1987; Katz et al, 1993; Muller and Nicholls, 1974; Koerber and Mendell, 1991; Mennerick and Zorumski, 1995; Davis, 1995; Reyes et al, 1998; Koester and Johnston,

\*To whom correspondence should be addressed. y.goda@ucl.ac.uk or t.branco@ucl.ac.uk.

The authors declare no competing financial interests.

2005). However, this simple relationship is not universal; for example, inputs on the same target can exhibit considerable variability (Jack et al, 1981; Redman and Walmsley, 1983; Walmsley, et al 1988; Redman, 1990; Hessler et al, 1993; Dobrunz and Stevens, 1997; Huang and Stevens, 1997), and in the limiting case of autaptic cell cultures, release probability can be highly non-uniform (Rosenmund et al, 1993; Murthy et al, 1997; Slutsky et al, 2004; Granseth et al, 2006). Thus, release sites from a single axon can have variable  $p_r$ , even when making contact on the same postsynaptic neuron. Aside from signaling mechanisms specific to the identity of the postsynaptic cell, there must be other factors contributing to the setting of release probability. At present, it is not known what these factors might be. Moreover, the potential functional relevance of  $p_r$  non-uniformity in the connection between two cells remains to be established.

In the present study we combine the use of simple networks of dissociated hippocampal cultured neurons with fluorescence imaging, electrophysiological recordings and ultrastructural analysis to establish the cellular principles used by synapses to define their basal release probability. We find that despite high overall variability, synapses from single axons contacting one dendritic tree have highly correlated release probabilities when they converge on the same branch of the dendrite. Furthermore,  $p_r$  homeostatically adapts both to the number of synapses in the branch and to selective increases in postsynaptic activity. This organization of  $p_r$  can be disrupted not only by global but also by local activity manipulations. Our findings suggest that  $p_r$  is set according to the local level of dendritic depolarization.

## Results

### Release probability is dendritically segregated

Using sparse cultured networks that permit a detailed characterization of individual synapses in an identified connection, we first examined  $p_r$  across the dendritic trees of single pyramidal neurons. Cells were filled with Alexa-dyes and synaptic contact points identified using FM4-64. To measure  $p_r$  at individual synapses, we evoked synaptic activity with field stimulation and imaged fluorescence loss due to vesicle exocytosis from the FM-dye-labeled synapses, where the rate of fluorescence decay is proportional to  $p_r$  (Zakharenko et al, 2001) (Fig. S1). Consistent with previous reports (Murthy et al, 1997; Slutsky et al, 2004)  $p_r$  had a broad and skewed distribution with an average median of  $0.22 \pm 0.03$ , and mean CV (coefficient of variation) of  $0.66 \pm 0.06$  ( $n = 12$  cells). To address what underlies this high variability of release probabilities, we then carried out a detailed analysis of  $p_r$  distribution. To do this, we first computed the absolute  $p_r$  difference between each synapse in a given cell and all other synapses from the same cell. This yielded a mean absolute  $p_r$  difference of 0.19, a value which was similar to that expected by random sampling of the measured  $p_r$  distribution (0.18,  $P = 0.8116$ ). We next normalized  $p_r$  differences for each synapse pair by the standard deviation of each cell, to generate a measure that allowed us to quantify the magnitude of the similarity between any two synapses in a given cell. This gave a mean difference of  $1.27 \pm 0.20$  SDs for all cells analyzed. Using this measure, we then analyzed the spatial distribution of  $p_r$  along the dendrites, by computing the average  $p_r$  difference between all synapses on single dendritic branches. We found that even for single branches

there was a large variability in release probability (mean difference =  $1.33 \pm 0.04$  SDs, not different from global mean difference,  $P = 0.4449$ ;  $CV = 0.61 \pm 0.06$ , not different from global CV,  $P = 0.5576$ , Fig. 1A, C). This finding is in accordance with previous ultrastructural data from native hippocampal tissue, where the size of presynaptic terminals onto dendritic branches is highly non-uniform (Harris and Sultan, 1995). Next, using whole-cell patch clamp, we stimulated target neurons and measured  $p_r$  at all synapses on the axonal arbor of single cells. Again, we found a large variability for synapses in individual axonal branches (mean difference =  $1.27 \pm 0.06$  SDs, not different from global mean difference,  $P = 0.4792$ ;  $CV = 0.69 \pm 0.09$ , not different from global CV,  $P = 0.7945$ ,  $n = 5$  cells, Fig. 1B, C). Furthermore, no relationship was found between  $p_r$  and distance to the soma along the dendrite or the axon (Fig. S2A). Interestingly, a small but significant negative correlation was found between synaptic density and release probability of synapses along a dendrite ( $R = -0.38$ ,  $P = 0.0351$ , Fig. S2B), although no such relationship was found for synapses along the axon.

To remove the potential sources of variability on  $p_r$  arising from examining a mixed population of synapses with different neuronal sources or targets, we next restricted our analysis to synapses connecting two neurons. Excitatory post-synaptic currents (EPSCs) were recorded with paired whole-cell patch clamp, and synaptic contact points identified using FM4-64 and Alexa dye-fills of axons and dendrites (Fig. 1D, E). On average, we detected  $8 \pm 5.4$  (SD) contact points between two cells with the culture conditions used. This is comparable to findings in intact tissue from ultrastructural analysis of multiple synapses found in connections between stratum radiatum-CA1 pyramids (Sorra and Harris, 1993) and CA1 and CA3 pyramidal cells-interneurons (Biro et al 2005, Wittner et al 2006), and from quantal analysis of excitatory connections onto CA1 pyramids (Larkman et al, 1997). Even in this reduced synaptic population  $p_r$  had a broad and skewed distribution with an average median of  $0.22 \pm 0.04$  and mean CV of  $0.51 \pm 0.13$  ( $n = 7$  pairs, Fig. 1F, G). The average absolute  $p_r$  difference between all synapses of a given connection was  $0.19 \pm 0.01$ , not different from the value expected by random sampling ( $0.17$ ,  $P = 0.6383$ ), corresponding to  $1.29 \pm 0.07$  SDs. We then repeated the branch specific spatial analysis as above for both axons and dendrites. We found that while  $p_r$  could be very different for synapses made along short segments of axons contacting different dendrites (mean difference =  $1.34 \pm 0.10$  SDs, not different from global mean difference,  $P = 0.8652$ ;  $CV = 0.48 \pm 0.09$ , not different from global CV,  $P > 0.9999$ ),  $p_r$  was very similar for synapses that shared the same dendritic branch (mean difference =  $0.44 \pm 0.07$  SDs, significantly different from synapses made on different dendrites from the same axon,  $P < 0.0001$  and from global mean difference,  $P < 0.0001$ ;  $CV = 0.12 \pm 0.04$ , significantly different from global CV,  $P = 0.0007$ , Fig. 2A-C). To confirm that  $p_r$  is segregated in a branch specific manner, we analyzed release probability of synapses separated by dendritic branch points, and found that in these cases  $p_r$  is markedly different (mean difference =  $1.52 \pm 0.26$  SDs,  $P < 0.0001$  compared with synapses made exclusively on the parent or daughter branch, Fig. S3). We also analyzed recycling pool sizes and found that this parameter exhibited dendritic homogeneity similarly to  $p_r$  (Fig. S4). Furthermore, release probability displayed a strong negative correlation with the number of synapses that the axon made on the dendritic branch ( $R = -0.53$ ,  $P < 0.0001$ , Fig. 2D), but not with the number of synapses along an axon contacting different dendrites ( $R = 0.01$ ,  $P =$

0.9349). These observations suggest that for single inputs,  $p_r$  is not randomly distributed, but rather, release probability is segregated at the level of individual dendrites.

### Spatial analysis of $p_r$ at the ultrastructural level

We next examined the spatial distribution of  $p_r$  using ultrastructural analysis, where we could unequivocally identify single synapses and the axonal and dendritic processes they belong to at high resolution. To measure release probability we directly counted the number of vesicles exocytosed in response to a defined number of action potentials (APs). This relied on FM1-43 photoconversion to distinguish vesicles labeled with FM-dye after exo/endocytosis, which appear dark in electron micrographs, from non-labeled vesicles (Harata et al, 2001; Schikorski and Stevens, 2001; Darcy et al, 2006). Synapses were FM1-43-loaded using field stimulation (30 APs, 1 Hz), identified at fluorescence level, and subsequently photoconverted, embedded and serially sectioned (Fig. 3A, C-G). Labeled synapses ( $n = 31$  from 4 cultures) had a median total pool size of 296 vesicles (interquartile range, IQR = 306), and a median  $p_r$  of 0.37 (IQR = 0.75). Using this synapse population, we analyzed the spatial distribution of  $p_r$  by examining all cases where synapses i) shared the same axon branch but different dendrite, or ii) shared the same axon branch and same dendrite. Consistent with our fluorescence measurements, synapses made onto the same dendrite had very similar  $p_r$  (mean difference =  $0.31 \pm 0.14$  SDs), while those contacting different dendrites had highly variable release probabilities (mean difference =  $1.51 \pm 0.66$  SDs,  $P = 0.0438$ , Fig. 3B).

### $P_r$ responds homeostatically to increased dendritic activity

Taken together, our fluorescence and ultrastructural observations demonstrate that in a connection between two neurons, neighboring synapses on the same dendritic segment have very similar release probabilities, whereas no such relationship is seen between  $p_r$  and the disposition of boutons along the axon. Moreover,  $p_r$  is negatively correlated with the number of synapses made by the axon onto the dendrite. These findings suggest that some form of dendritically-coordinated adaptation contributes to the local setting of basal release probability. We next sought to test this hypothesis by first establishing a condition that drives homeostatic changes in  $p_r$  and then examining the contribution of dendritic activity in altering  $p_r$ . We increased network activity by delivering APs at 1-2 Hz for 2 h, and estimated release probability with whole-cell paired recordings (Fig. 4A). This manipulation resulted in a  $23 \pm 5\%$  increase in the paired pulse ratio (PPR) of EPSC amplitudes (control PPR =  $0.71 \pm 0.05$ ,  $n = 16$ ), consistent with a decrease in release probability ( $t$ -test,  $P = 0.0394$ ,  $n = 8$ , Fig. 4B). To compare  $p_r$  between control and stimulated cultures by quantal analysis, we recorded EPSCs under low  $p_r$  conditions by adjusting the extracellular  $\text{Ca}^{2+}/\text{Mg}^{2+}$  ratio to the point where failures of evoked responses could be detected (control failure rate =  $32 \pm 3\%$ ,  $n = 7$ ). This decreased the mean quantal content (control mean quantal content =  $1.19 \pm 0.09$ ), and produced clearly quantized evoked responses (Fig. 4C right, inset), that when converted to a frequency histogram, appeared as well-defined peaks. For each cell we also recorded spontaneous miniature EPSCs and baseline noise, and an analysis of the histograms was performed as in Larkman et al (1997). In all cells examined, clear, equally spaced peaks were identified, with the first and second peaks matching the baseline noise and mEPSC histograms, respectively (Fig 4C). We then fitted a compound binomial model to the

identified peaks to extract mean release probability, number of active release sites (N) and  $p_r$  CV. Control values were  $p_r = 0.16 \pm 0.04$  (the reduced extracellular  $\text{Ca}^{2+}/\text{Mg}^{2+}$  compared to our FM-dye experiments yields a lower  $p_r$  estimate),  $p_r$  CV =  $0.50 \pm 0.15$  and  $N = 11 \pm 0.5$ , in good agreement with the values obtained from FM-dye destaining. Analysis of stimulated cultures showed a  $70.0 \pm 11$  % decrease in  $p_r$  ( $P = 0.0424$ ,  $n = 4$ ), with no change in N ( $P = 0.3420$ , Fig 4D). Therefore, release probability responds homeostatically to elevated network activity arising from the 2 h stimulation protocol.

In order to determine whether homeostatic down-regulation of  $p_r$  is specifically dependent on dendritic activity and how presynaptic activity might contribute to this process, we selectively silenced postsynaptic excitatory activity by stimulating the network in the presence of glutamate receptor blockers. We found no compelling evidence for neurotransmitter release modulation by presynaptic AMPA or NMDA receptors in our cultures (Fig. S5), and thus this manipulation eliminates dendritic activity while allowing normal presynaptic function. Block of excitatory receptors significantly abolished the increase in PPR of evoked responses (t-test,  $P = 0.0377$ ,  $n = 6$ , Fig. 4B). Moreover, quantal analysis ( $P = 0.0420$ ,  $n = 4$ ) revealed a tendency for release probability to be higher than in control, indicative of a homeostatic adaptation to reduced activity despite enhanced presynaptic stimulation (Fig. 4D). As with the control activity alone condition, no changes were detected in the number of release sites. These results therefore, strongly suggest that homeostatic adjustment of  $p_r$  depends on postsynaptic activation, and that release of neurotransmitter from the presynaptic terminal by itself is not sufficient to down-regulate  $p_r$ . Given that our stimulation protocol evokes spikes in both pre and postsynaptic cells, these data also indicate that action potential firing and back propagation alone cannot account for the observed decrease in  $p_r$ .

### Local homeostasis underlies $p_r$ variability

What might give rise to the observed heterogeneity of  $p_r$ ? This could be explained if homeostatic regulation of release probability is implemented locally, where spatially-distinct parts of the dendritic tree receiving different inputs experience different activity levels and consequently have synapses with dissimilar  $p_r$ . In this case, upon forcing inputs to the dendrite to be uniform across the entire dendritic tree, the variability in  $p_r$  should become very small. To test this prediction, we used two different experimental conditions to uniformly modulate input to dendrites (Fig. 5A). First, we blocked excitatory and inhibitory postsynaptic receptors for 24 h thereby rendering all dendrites silent. Second, we uniformly increased dendritic depolarization by raising the KCl concentration in the culture media while blocking postsynaptic receptors for 24 h. For each case, we then repeated the  $p_r$  measurements at individual synapses between identified cell pairs using whole-cell patch clamp and FM-dye imaging. Under both conditions the variability of release probability was greatly reduced (CV =  $0.17 \pm 0.03$ ,  $P = 0.0087$ ,  $n = 5$  for activity block and CV =  $0.19 \pm 0.06$ ,  $P = 0.0303$ ,  $n = 5$  for KCl, Fig. 5B, C), while  $p_r$  changed homeostatically in opposite directions (median  $p_r = 0.41$ , IQR = 0.16,  $P < 0.0001$  for activity block,  $p_r = 0.07$ , IQR = 0.06,  $P < 0.0001$  for KCl, Fig. 5B, C). Moreover, in accordance with reduced  $p_r$  variability, the average absolute  $p_r$  difference between all synapses in a connection decreased to 0.12

$\pm 0.01$  for block, and  $0.03 \pm 0.01$  for KCl (significantly different from control,  $P < 0.0001$  and  $P < 0.0001$ , respectively).

We then repeated the branch specific spatial analysis of  $p_r$ . Given that under these conditions there was a marked decrease in the standard deviation of the  $p_r$  distribution, to allow comparisons to control conditions we calculated mean  $p_r$  differences as before, but then expressed them as a fraction of the control population SD. Consistent with the overall increase in release probability uniformity, mean  $p_r$  differences between synapses belonging to different dendritic branches decreased to  $43 \pm 4\%$  of control for block, and to  $3 \pm 0.4\%$  of control for KCl ( $P < 0.0001$  and  $P < 0.0001$ , respectively), and were not significantly different from  $p_r$  differences between synapses in the same dendritic branch ( $P = 0.2660$  for block and  $P = 0.1314$  for KCl, see Fig. 5D-F). Furthermore, the relationship between  $p_r$  and the number of synapses made on the dendrite was lost ( $R = -0.03$ ,  $P = 0.8746$  and  $R = -0.45$ ,  $P = 0.0804$ , respectively, Fig. 5G). The same increase in similarity was found for recycling pool sizes (Fig. S4). The heterogeneity of  $p_r$ , therefore, is a consequence of non-uniformity of dendritic activity.

To directly monitor local modulation of  $p_r$ , we carried out experiments where we increased synaptic activity to induce homeostatic down-regulation of  $p_r$ , but restricted stimulation to a subset of synapses in a dendritic branch (Fig. 6A, B). We then measured  $p_r$  by labeling all synapses with FM-dye (30 APs, 1 Hz, Fig. 6C, D). After 2 h of localized stimulation, release probability of the stimulated synapses was  $41 \pm 4\%$  lower when compared to unstimulated synaptic neighbors ( $P < 0.0001$ ), and this effect was blocked by CNQX and APV ( $P = 0.1872$ , Fig. 6D, E). Altogether, these results indicate that the homeostatic control of  $p_r$  is implemented locally.

Our spatial analysis of  $p_r$  shows that a high degree of  $p_r$  similarity in individual dendritic branches occurs only if synapses come from the same presynaptic cell. This implies that  $p_r$  homeostasis is triggered by the increased level of postsynaptic activity which is coincident with presynaptic activation. In this case, synapses in a dendrite that belong to the same axon are activated synchronously, and they would adapt to similar levels of dendritic depolarization. On the other hand, synapses from different inputs that are likely to be active asynchronously would produce different depolarization levels, and consequently they would generate different  $p_r$  adaptations. To provide experimental support for this hypothesis, we used DIC and FM-dye images to trace the axons of synapses analyzed in our local activity manipulation experiments (Fig. S6). We found that in all cases, synapses from different presynaptic cells were found in the stimulated area (Fig. 6F, top half), and that after stimulation, the CV of release probability was significantly reduced to the level of synapses from the same input onto a single dendritic branch ( $P < 0.0001$ , Fig. 6H). This shows that if two inputs from different presynaptic cells are forced to release synchronously, they acquire similar release probabilities. In some cases, synapses from the same axon were found both in the stimulated and non-stimulated area of the same dendritic branch (Fig. 6F, bottom half). Only the stimulated group showed a decrease in  $p_r$  ( $P = 0.0038$ , Fig. 6G), strongly supporting the argument that the  $p_r$  similarity found for synapses from the same input onto the same branch results from synchrony of their activation. Taken together, these

observations suggest that release probability is down-regulated by a coincidence detection mechanism that requires neurotransmitter release and dendritic depolarization.

## Discussion

In this study, we combined fluorescence imaging, electrophysiological and ultrastructural methods in dissociated hippocampal cultured neurons to address the determinants of release probability at single synapses. Initially, we considered the spatial organization of  $p_r$ . Although the  $p_r$  distribution was broad with high CV in pairs of synaptically connected cells, an analysis of spatial distribution at the level of axonal and dendritic branches showed that synapses made on the same branch of the dendrite had a high degree of similarity. However, when one axon branch contacted different dendritic branches, variability was not significantly different from what might be expected by chance. Because our analysis was always restricted to segments of axons in between two branch points, failures of action potential propagation would not provide a satisfactory explanation for the observation of high  $p_r$  variability in the axon. This basic organizational principle of  $p_r$  was also supported by two further lines of evidence. First, a spatial relationship similar to that for release probability was established for the total recycling pool size, a known correlate of  $p_r$ . Second a spatial analysis of  $p_r$  at EM level also showed dendritic clustering of release probabilities. This suggests that release probability of synapses from a given axon is biased towards acquiring a particular value at individual dendritic branches. Our spatial analysis also revealed an additional salient feature:  $p_r$  is inversely correlated with the number of synapses made on the same branch of the dendrite. Since action potential firing in cultured neurons is likely to be random due to a lack of external input, the level of activity of any given part of the dendritic tree should be proportional to the number of synapses. Thus, the relationship between synapse number and  $p_r$  can be viewed as a relationship between activity in the dendrite and release probability. The fact that no such correlation was found for synapses along an axon contacting different dendrites could not be explained by a systematic difference in disposition or density of boutons, since the inter-synaptic distance and process length were not different between the two cases. Collectively, these data imply that release probability homeostatically adapts to the level of activity in the dendrite, and since different branches have different mean  $p_r$ s, such regulation must be implemented locally. A negative correlation between  $p_r$  and synapse density was also found for all synapses along a dendrite, regardless of their origin. However, this correlation was weaker and less steep than for synapses arising from the same input, in line with our argument that the negative feedback regulation we describe is dependent on postsynaptic activation that is coincident with presynaptic activation.

We used paired whole-cell recordings and three different estimates of  $p_r$  to explore homeostatic adaptations of release probability. Whereas continuous low-frequency delivery of action potentials to the whole network caused an expected significant decrease in  $p_r$ , eliciting action potentials while blocking excitatory synaptic transmission uncoupled pre and postsynaptic activity and enabled us to investigate the locus of homeostatic plasticity induction. Importantly, stimulating the network in the presence of glutamate receptor blockers represents a different condition to blocking receptors alone. While in the former, evoked neurotransmitter release still occurs, in the latter, the lack of excitatory input

abolishes network AP firing. The fact that in the presence of synaptic blockers, release probability did not decrease despite enhanced axonal activity, indicates that a direct action of neurotransmitter on the presynaptic terminal or the average level of depolarization in the presynaptic compartment are not sufficient for homeostatic adaptation of  $p_r$ . Rather, it supports the view that neurotransmitter has to depolarize the dendrite for homeostatic mechanisms to be activated.

To address the local nature of the relationship between  $p_r$  and dendritic depolarization, we forced spatially uniform depolarization levels along the dendritic tree by either blocking excitatory and inhibitory synaptic input, or by increasing the culture medium KCl concentration while blocking postsynaptic receptors. Maintaining these manipulations for 24 h resulted in a homeostatic change in release probability in which synapses had very similar  $p_r$  regardless of their spatial arrangement. Importantly, these manipulations do not represent extremes of membrane potential displacement. Given that, in our system, neurotransmitter release occurs at a rate of ~5 Hz, neurons will spend the majority of time near resting potential. Completely blocking synaptic activity will thus only eliminate the small membrane depolarizations brought about by single EPSPs, leaving the cell permanently at resting potential. This is clearly a very mild change to the membrane potential, well below changes brought about by inhibition, for example. The KCl manipulation depolarizes the soma by ~15 mV, as measured by whole-cell recording, which while being stronger than activity block, is well within the limits of physiological relevance. Therefore, the type of  $p_r$  regulation we observe is very sensitive to small changes in postsynaptic membrane potential, and that the resulting similarity of  $p_r$  across synapses does not represent the consequence of driving synaptic strength to the end of the dynamic range by extreme changes in membrane potential. Furthermore, the finding that under these conditions CV and similarity values for synapses in the same dendrite are the same as in control, suggests that the changes elicited by the manipulations are within physiological range and are not taking the system to artifactual limits.

The observed loss of release probability variability upon spatially uniform manipulations of the postsynaptic membrane potential strongly links the  $p_r$  heterogeneity with the non-uniformity in inputs to the dendritic tree, thus providing additional support to the idea that the homeostatic response of release probability is implemented at a local level. Furthermore, under these conditions, the inverse relationship between release probability and the number of synapses on the same branch of the dendrite is lost. This is presumably because postsynaptic receptor blockers prevent each synapse from having an impact on dendritic activity, and each individual synapse will adapt to the same average membrane potential. Therefore, in order for a relation between synapse number and  $p_r$  to be established, the difference in the number of synapses has to be converted into a difference in local dendritic activity. Importantly, the local regulation of release probability was further confirmed by selectively stimulating a small group of synapses for 2 h, which produced a compensatory decrease in  $p_r$  that was confined to the stimulated area, as was the corresponding increase in similarity.

One possible explanation for the observation of spatial  $p_r$  segregation is a developmental one. Given that  $p_r$  is developmentally regulated, being initially high and decreasing with



maturation (Reyes and Sakmann, 1999, Chavis and Westbrook, 2001), synapses of the same age are expected to have similar release probabilities. In such a case, spatial segregation would reflect developmental age, where synapses in the same branch have been formed at the same time. Although efforts were made to ensure the overall maturity of our cultures (Fig. S7), we cannot exclude that different synapses are at different stages of maturation, and that this contributes to the observed spatial distribution. However, the inverse correlation between the number of synapses on the dendrite and  $p_r$ , and the changes in  $p_r$  and its variability imposed by different activity manipulations, highlight the link between postsynaptic activity and release probability and indicate that developmental maturity is not the main variable determining  $p_r$  in our system.

A recent study in L2/3 cortical cells has suggested that synapses onto the same postsynaptic target adopt the same  $p_r$ , regardless of their position in the dendritic tree. In their study they estimated an overall CV of  $\sim 0.20$  (Koester and Johnston, 2005). Despite the apparent contradiction with our results, their finding can actually be readily explained by the model of  $p_r$  regulation we propose. Assuming there is no systematic bias in the distribution of synapses *in vivo*, the high and uniform density of synaptic contacts along a given branch will produce, on average, the same activity level. Synapses from a single axon will therefore operate on a similar activity background irrespective of their location in the dendritic tree, and our model predicts that they will adapt to a release probability representing this background and the depolarization caused by their activation. Given that such synapses share the same presynaptic cell, their activation rate will be the same, and therefore would be expected to develop similar release probabilities. We also believe that our model can fully account for the wide  $p_r$  variability observed in autaptic synapses. Given that pure autaptic cultures are isolated from any other inputs, they seldom fire action potentials spontaneously, and thus synaptic activity is restricted to spontaneous neurotransmitter release occurring stochastically in space and time. Given this scenario, and in view of our suggestion that  $p_r$  modulation is restricted to activated synapses, the reported variability in autapses is to be expected.

Previous studies have reported homeostatic regulation of  $p_r$  in response to inactivity (Murthy et al, 2001; Bacci et al, 2001; Burrone et al, 2002; Thiagarajan et al, 2005; Wierenga et al, 2006), and this is thought to maintain stability in the network whilst permitting efficient Hebbian learning (Burrone and Murthy, 2003). Likewise, we suggest here that homeostatic setting of basal release probability at individual synapses ensures that each synapse is optimally placed to undergo changes such as those observed in short- and long-term plasticity (Stevens and Wang, 1994). To provide a theoretical basis for this, we simulated a CA1 pyramidal cell receiving a variable number of excitatory synaptic inputs stimulated synchronously. Although in our simplified culture system and some types of connections in the intact hippocampus this corresponds to one axon making multiple contacts in one dendrite, in other cases this would be equivalent to synchronous and layered inputs into the dendritic tree. We found that while synaptic output increased linearly with increases in release probability when one synapse was stimulated, synchronous activation of more than one synapse led to sub-linear responses as  $p_r$  approached one, due to a reduction in the driving force and shunting (Fig. S8). Therefore, to prevent saturation of synaptic current, synapses match their release probability to the level of activity on the postsynaptic target.

Since each dendrite can behave as a different electrotonic compartment (Rabinowitch and Segev, 2006) and is likely to receive different inputs, this mechanism must be implemented locally to be effective. In contrast to more traditional forms of synaptic homeostasis that are thought to represent a cell-wide phenomenon (Turrigiano and Nelson, 2000), theoretical prediction (Rabinowitch and Segev, 2006) and recent experimental evidence also point to a local homeostatic control of synaptic strength (Ju et al, 2004; Liu, 2004; Sutton et al, 2006). Aside from preventing synaptic saturation, such a mechanism could function to match the strength of synaptic input to the degree of excitability of each dendritic compartment (Polsky et al, 2004).

Collectively, our results indicate that individual synapses must monitor activity of their neighbors and continually adjust their release probability. One important issue that remains to be fully characterized is the extent of the spatial spread of this feedback regulation, which will be dependent on the underlying mechanism. Given the branch specific distribution of release probability and the triggering of  $p_r$  homeostasis with increased depolarization, even in the presence of synaptic blockers, we suggest that a dendritic depolarization-dependent release of a feedback substance might be responsible for  $p_r$  homeostasis. Since transient synaptic potentials spread very efficiently through short dendritic branches but decay considerably with branching, a depolarization based  $p_r$  regulation would be expected to mainly affect synapses in the same branch of the dendrite. This could be implemented by known retrograde messengers involved in feedback regulation of release probability, such as the ones described for the *Drosophila* neuromuscular junction (Frank et al, 2006; Davis, 2006), and those thought to underlie both the target-cell dependence of  $p_r$  and forms of short-term plasticity or LTD (Duguid and Sjostrom, 2006). We cannot, however, exclude the possibility that the spatial spread is in the range of a few microns, something that could be mediated by entry of calcium via GluR2-lacking AMPA receptors, for example. Importantly, our model proposes that this form of  $p_r$  homeostasis only affects synapses that have released neurotransmitter. This implies that apart from a retrograde messenger, some form of coincidence detection is also needed, such as activation of pre or postsynaptic mGluRs by the released glutamate, for example (Conn and Pin 1997).

The release probability homeostasis model we propose differs from more classic forms of homeostasis (Turrigiano and Nelson 2000), not only because it appears to be local, but also because it seems to act over a different timescale. Although the direction of change is the same as previously described for presynaptic changes, classic homeostasis is thought to occur over hours/days, whereas our 2 h activity manipulations were sufficient to change release probability. Furthermore, the finding that this mechanism drives  $p_r$  heterogeneity in the resting state indicates that this mode of regulation operates with basal, random, spontaneous activity, and is not dependent on some sort of threshold or timed activity. We thus propose that this feedback regulation of  $p_r$  acts within a very short integration window, being rapidly activated by each single quanta of neurotransmitter released, and continuously operating on the background to quickly adapt release probability to the dendritic environment. This type of model is similar to what Frank et al (2006) found for the *Drosophila* NMJ, and consistent with that described by Sutton et al (2006) for postsynaptic scaling. In this way, this mechanism is also different from classic Hebbian plasticity, like LTD, for example, where particular stimulus conditions have to be met for such plasticity to

develop. It is worth noting that LTD is, in itself, a form of synaptic homeostasis, and it might be that both forms of plasticity are part of one continuum, the major difference between them being the rate at which voltage perturbations of the membrane potential are imposed.

## Materials and Methods

### Cell culture

Hippocampal neurons were obtained from P0-P1 rat pups and plated at low density onto an astrocyte feeder layer and maintained in Neurobasal-based culture media. Cells were used for experiments at 10-15 days *in vitro*.

### Electrophysiology

Paired whole-cell recordings were obtained with pipettes (3-5 M $\Omega$ ) containing (in mM): 115 KMeSO<sub>4</sub>, 5 KCl, 4 NaCl, 10 HEPES, 0.5 CaCl<sub>2</sub>, 10 creatine phosphate, 2 MgATP, 2 Na<sub>2</sub>ATP, 0.3 Na<sub>3</sub>GTP, 10 glutamic acid (pH 7.20) and 100  $\mu$ M Alexa 488 or 500  $\mu$ M Alexa 350 hydrazide (Molecular Probes). The external solution contained (in mM): 125 NaCl, 5 KCl, 10 D-glucose, 10 HEPES with 2 CaCl<sub>2</sub> and 1 MgCl<sub>2</sub> unless otherwise stated (pH 7.30). Recordings were made at  $34 \pm 1^\circ\text{C}$  in the presence of 10  $\mu$ M picrotoxin to isolate excitatory currents and discarded if the access resistance was  $> 30 \text{ M}\Omega$  (not compensated). Data were acquired with a Multiclamp 700B (Axon Instruments), filtered to 10 kHz and digitized at 50 kHz. APs were elicited in current clamp by injecting 1 ms 0.5 – 1 nA current pulses and the postsynaptic cell was voltage-clamped usually at -70 mV (corrected for a junction potential of 10 mV). For paired pulse experiments, inter-pulse interval was 50 ms and a minimum of 30 sweeps were acquired at 0.1 Hz. For recordings in low Ca<sup>2+</sup> the stimulation frequency was 1 Hz and 100 - 300 traces were obtained. Data were analyzed with Neuromatic software and only monosynaptic responses were considered (mean latency  $1.94 \pm 0.15 \text{ ms}$ , 20-80% rise-time  $472 \pm 30 \mu\text{s}$ ). In low Ca<sup>2+</sup> conditions, events were considered to be evoked EPSCs if they fell within the time period defined by the averaged evoked EPSC time course. EPSC integral histograms were constructed using small bins and smoothed with a binomial algorithm in Igor Pro 4.06 (WaveMetrics). The position of the peaks was identified by Gaussian fitting (Larkman, 1997). For fitting of a compound binomial model, Monte Carlo simulations of quanta release with varying numbers of release sites and  $p_r$  distributions with different CVs were performed in Matlab 7.1 (Mathworks), and the distribution that best fitted the data selected.

### Imaging

Epifluorescence images were acquired on an inverted Olympus IX71 microscope using a Micromax cooled-CCD camera (Princeton Instruments) driven by Metamorph software (Universal Imaging). Synapses were labeled with FM4-64 by incubating cultures with 10  $\mu$ M of dye in extracellular solution containing 90 mM KCl, CNQX (20  $\mu$ M) and APV (50  $\mu$ M) for 1 min at room temperature. Following this, neurons were rinsed in normal extracellular solution containing FM4-64 for a further minute, to allow completion of endocytosis. Cells were then washed in extracellular solution with 0.5 mM Ca<sup>2+</sup> and 10 mM Mg<sup>2+</sup> to minimize dye-loss from spontaneous release and Advasep-7 (1 mM, Biotium) was included for the first minute of the washing procedure to assist with FM-dye removal from

membranes. For experiments in single cells, neurons were filled with Alexa dye via a patch pipette, and FM-dye destaining evoked either by field stimulation in a custom made chamber or via the patch pipette, as referred in the text. For connected cells, after a paired recording was obtained and neuronal processes were filled with Alexa dye, a region of interest that included FM-labeled puncta that were likely synaptic contact points between the recorded neurons was chosen, and FM-dye destaining was monitored by acquiring images every minute at room temperature. During stimulation CNQX (20  $\mu$ M) and APV (50  $\mu$ M) were used to prevent recurrent stimulation of the network. The fluorescence of each FM-dye punctum was quantified using custom written routines in Igor Pro 4.06 (WaveMetrics) and Matlab 7.1 (Mathworks) and  $p_r$  was calculated from the estimated recycling pool size and destaining kinetics (Fig. S1). For release probability comparisons between synapses,  $p_r$  difference was calculated between each synapse and all other synapses in the branch or cell, depending on the experiment, and this value averaged. Absolute differences were normalized to the  $p_r$  SD of each cell. In an initial set of experiments, the maturity of the synapse population under study was assessed by co-labeling synapses with FM4-64 and an antibody raised against the extracellular domain of GluR2 (Chemicon, see Fig. S5).

### Electron microscopy

Synaptic vesicles were labeled with a fixable form of 10  $\mu$ M FM1-43 (FM1-43FX, Molecular Probes) and washed as above. Neurons were fixed and FM-dye was photoconverted in the presence of diaminobenzidine (1 mg/ml), before being prepared for electron microscopy as previously described (Darcy 2006). Serial sections of embedded neurons were placed on formvar coated slot grids and viewed using an electron microscope (Phillips CM10). Images were acquired using a 1392 x 1040 cooled CCD camera (Roper Scientific). Synapses and neuronal processes were reconstructed using graphics software (Xara Xtreme) to establish the precise spatial arrangement of axons and dendrites. Photoconverted vesicles have a dark lumen and could be readily distinguished from unstained vesicles using previously-described methods (Darcy 2006). For consistency with the fluorescence measurements, the ultrastructural measure of  $p_r$  difference was restricted to synapses < 10  $\mu$ m apart (the 90% confidence interval of synapse separation found for the fluorescence-based analysis). 3-d reconstructions of processes and presynaptic terminals were made using specialist software ('Reconstruct', J. Fiala, available at <http://synapses.bu.edu>).

### Activity manipulations

For long-term manipulation of activity, cells were placed in a custom-made chamber and stimulated (2 ms, 5 V pulses, 1-2 Hz field stimulation) while maintaining the culture in the incubator. When required, drugs were added to the culture medium (20  $\mu$ M CNQX, 50  $\mu$ M APV, 20  $\mu$ M bicuculline). All data were obtained in parallel on treated and age-matched sister control cultures.

### Statistics

To compare data sets, non-parametric tests (Mann-Whitney U-test, Wilcoxon rank sum test or  $\chi^2$  test) were used unless otherwise indicated. Tests for normality and comparisons of distributions were made using Kolmogorov-Smirnov tests. Pearson r-test or Spearman r-test

were used for correlation analysis. Monte Carlo simulations were done by random sampling the theoretical distribution fit to the data. Statistical significance was assumed when  $P < 0.05$ . In figures, \* indicates  $P < 0.05$ , \*\* indicates  $P < 0.01$  and \*\*\* indicates  $P < 0.001$ . Values in text represent mean  $\pm$  s.e.m for normally-distributed data and median and interquartile range (IQR) for data which did not meet the criteria for normality.

## Supplementary Material

Refer to Web version on PubMed Central for supplementary material.

## Acknowledgments

We thank A. Roth, M. London, J. Sjöström and D. Attwell for critical comments on a early version of the manuscript, and B. Clark, M. Häusser and M. London for helpful discussions. We also thank L. Collinson for serial sectioning, L. Yu for technical assistance and A. Roth for help with the simulations. This work was supported by the Wellcome Trust 4 year PhD Programme in Neuroscience at UCL to T.B., and a Medical Research Council and National Institutes of Health grant to Y.G.

## References

- Atwood HL, Bittner GD. Matching of excitatory and inhibitory inputs to crustacean muscle fibers. *J Neurophysiol.* 1971; 34:157–170. [PubMed: 4322251]
- Bacci A, Coco S, Pravettoni E, Schenk U, Armano S, et al. Chronic blockade of glutamate receptors enhances presynaptic release and downregulates the interaction between synaptophysin-synaptobrevin-vesicle-associated membrane protein 2. *J Neurosci.* 2001; 21:6588–6596. [PubMed: 11517248]
- Bennett MR, Jones P, Lavidis NA. The probability of quantal secretion along visualized terminal branches at amphibian (*Bufo marinus*) neuromuscular synapses. *J Physiol.* 1986; 379:257–274. [PubMed: 2882019]
- Biró AA, Holderith NB, Nusser Z. Quantal size is independent of the release probability at hippocampal excitatory synapses. *J Neurosci.* 2005; 25:233–232. [PubMed: 15634786]
- Burrone J, Murthy VN. Synaptic gain control and homeostasis. *Curr Opin Neurobiol.* 2003; 13:560–567. [PubMed: 14630218]
- Burrone J, O'Byrne M, Murthy VN. Multiple forms of synaptic plasticity triggered by selective suppression of activity in individual neurons. *Nature.* 2002; 420:414–418. [PubMed: 12459783]
- Cooper RL, Harrington CC, Marin L, Atwood HL. Quantal release at visualized terminals of a crayfish motor axon: intraterminal and regional differences. *J Comp Neurol.* 1996; 375:583–600. [PubMed: 8930787]
- Chavis P, Westbrook G. Integrins mediate functional pre- and postsynaptic maturation at a hippocampal synapse. *Nature.* 2001; 411:317–321. [PubMed: 11357135]
- Conn PJ, Pin JP. Pharmacology and functions of metabotropic glutamate receptors. *Annu Rev Pharmacol Toxicol.* 1997; 37:205–237. [PubMed: 9131252]
- Darcy KJ, Staras K, Collinson LM, Goda Y. Constitutive sharing of recycling synaptic vesicles between presynaptic boutons. *Nat Neurosci.* 2006; 9:315–321. [PubMed: 16462738]
- Davis GW. Long-term regulation of short-term plasticity: a postsynaptic influence on presynaptic transmitter release. *J Physiol Paris.* 1995; 89:33–41. [PubMed: 7581297]
- Davis GW. Homeostatic control of neural activity: from phenomenology to molecular design. *Annu Rev Neurosci.* 2006; 29:307–323. [PubMed: 16776588]
- Del Castillo J, Katz B. Quantal components of the end-plate potential. *J Physiol.* 1954; 124:560–573. [PubMed: 13175199]
- Dobrunz LE, Stevens CF. Heterogeneity of release probability, facilitation, and depletion at central synapses. *Neuron.* 1997; 18:995–1008. [PubMed: 9208866]

- Duguid I, Sjöström PJ. Novel presynaptic mechanisms for coincidence detection in synaptic plasticity. *Curr Opin Neurobiol.* 2006; 16:312–322. [PubMed: 16713246]
- Frank CA, Kennedy MJ, Goold CP, Marek KW, Davis GW. Mechanisms underlying the rapid induction and sustained expression of synaptic homeostasis. *Neuron.* 2006; 52:663–677. [PubMed: 17114050]
- Frank E. Matching of facilitation at the neuromuscular junction of the lobster: a possible case for influence of muscle on nerve. *J Physiol.* 1973; 233:635–658. [PubMed: 4356843]
- Gasparini S, Migliore M, Magee JC. On the initiation and propagation of dendritic spikes in CA1 pyramidal neurons. *J Neurosci.* 2004; 24:11046–56. [PubMed: 15590921]
- Granseth B, Odermatt B, Royle SJ, Lagnado L. Clathrin-mediated endocytosis is the dominant mechanism of vesicle retrieval at hippocampal synapses. *Neuron.* 2006; 51:773–786. [PubMed: 16982422]
- Harata N, Ryan TA, Smith SJ, Buchanan J, Tsien RW. Visualizing recycling synaptic vesicles in hippocampal neurons by FM 1-43 photoconversion. *Proc Natl Acad Sci U S A.* 2001; 98:12748–12753. [PubMed: 11675506]
- Harris KM, Sultan P. Variation in the number, location and size of synaptic vesicles provides an anatomical basis for the nonuniform probability of release at hippocampal CA1 synapses. *Neuropharmacology.* 1995; 34:1387–1395. [PubMed: 8606788]
- Hessler NA, Shirke AM, Malinow R. The probability of transmitter release at a mammalian central synapse. *Nature.* 1993; 366:569–573. [PubMed: 7902955]
- Hines ML, Carnevale NT. The NEURON simulation environment. *Neural Comput.* 1997; 9:1179–1209. [PubMed: 9248061]
- Huang EP, Stevens CF. Estimating the distribution of synaptic reliabilities. *J Neurophysiol.* 1997; 78:2870–2880. [PubMed: 9405507]
- Jack JJ, Redman SJ, Wong K. The components of synaptic potentials evoked in cat spinal motoneurons by impulses in single group Ia afferents. *J Physiol.* 1981; 321:65–96. [PubMed: 6279826]
- Ju W, Morishita W, Tsui J, Gaietta G, Deerinck TJ, et al. Activity-dependent regulation of dendritic synthesis and trafficking of AMPA receptors. *Nat Neurosci.* 2004; 7:244–253. [PubMed: 14770185]
- Katz PS, Kirk MD, Govind CK. Facilitation and depression at different branches of the same motor axon: evidence for presynaptic differences in release. *J Neurosci.* 1993; 13:3075–3089. [PubMed: 8331385]
- Koerber HR, Mendell LM. Modulation of synaptic transmission at Ia-afferent fiber connections on motoneurons during high-frequency stimulation: role of postsynaptic target. *J Neurophysiol.* 1991; 65:590–597. [PubMed: 1646867]
- Koester HJ, Johnston D. Target cell-dependent normalization of transmitter release at neocortical synapses. *Science.* 2005; 308:863–866. [PubMed: 15774725]
- Larkman AU, Jack JJ, Startford KJ. Quantal analysis of excitatory synapses in rat hippocampal CA1 in vitro during low-frequency depression. *J Physiol.* 1997; 505:457–471. [PubMed: 9423186]
- Liu G. Local structural balance and functional interaction of excitatory and inhibitory synapses in hippocampal dendrites. *Nat Neurosci.* 2004; 7:373–379. [PubMed: 15004561]
- Maass W, Zador A. Dynamic stochastic synapses as computational units. *Neural Comput.* 1999; 11:903–17. [PubMed: 10226188]
- Mennerick S, Zorumski CF. Paired-pulse modulation of fast excitatory synaptic currents in microcultures of rat hippocampal neurons. *J Physiol.* 1995; 488:85–101. [PubMed: 8568668]
- Muller KJ, Nicholls JG. Different properties of synapses between a single sensory neurone and two different motor cells in the leech C.N.S. *J Physiol.* 1974; 238:357–369. [PubMed: 4366432]
- Murthy VN, Schikorski T, Stevens CF, Zhu Y. Inactivity produces increases in neurotransmitter release and synapse size. *Neuron.* 2001; 32:673–682. [PubMed: 11719207]
- Murthy VN, Sejnowski TJ, Stevens CF, Zhu Y. Heterogeneous release properties of visualized individual hippocampal synapses. *Neuron.* 1997; 18:599–612. [PubMed: 9136769]

- Pickard L, Noel J, Henley JM, Collingridge GL, Molnar E. Developmental changes in synaptic AMPA and NMDA receptor distribution and AMPA receptor subunit composition in living hippocampal neurons. *J Neurosci.* 2000; 20:7922–31. [PubMed: 11050112]
- Polsky A, Mel BW, Schiller J. Computational subunits in thin dendrites of pyramidal cells. *Nat Neurosci.* 2004; 7:621–627. [PubMed: 15156147]
- Rabinowitch I, Segev I. The interplay between homeostatic synaptic plasticity and functional dendritic compartments. *J Neurophysiol.* 2006; 96:276–283. [PubMed: 16554518]
- Redman S. Quantal analysis of synaptic potentials in neurons of the central nervous system. *Physiol Rev.* 1990; 70:165–198. [PubMed: 2404288]
- Redman S, Walmsley B. Amplitude fluctuations in synaptic potentials evoked in cat spinal motoneurons at identified group Ia synapses. *J Physiol.* 1983; 343:135–145. [PubMed: 6644615]
- Reyes A, Lujan R, Rozov A, Burnashev N, Somogyi P, et al. Target-cell-specific facilitation and depression in neocortical circuits. *Nat Neurosci.* 1998; 1:279–285. [PubMed: 10195160]
- Reyes A, Sakmann B. Developmental switch in the short-term modification of unitary EPSPs evoked in layer 2/3 and layer 5 pyramidal neurons of rat neocortex. *J Neurosci.* 1999; 19:3827–3835. [PubMed: 10234015]
- Robitaille R, Tremblay JP. Non-uniform release at the frog neuromuscular junction: evidence of morphological and physiological plasticity. *Brain Res.* 1987; 434:95–116. [PubMed: 2882823]
- Rosenmund C, Clements JD, Westbrook GL. Nonuniform probability of glutamate release at a hippocampal synapse. *Science.* 1993; 262:754–757. [PubMed: 7901909]
- Ryan TA, Reuter H, Smith SJ. Optical detection of a quantal presynaptic membrane turnover. *Nature.* 1997; 388:478–482. [PubMed: 9242407]
- Schikorski T, Stevens CF. Morphological correlates of functionally defined synaptic vesicle populations. *Nat Neurosci.* 2001; 4:391–395. [PubMed: 11276229]
- Slutsky I, Sadeghpour S, Li B, Liu G. Enhancement of synaptic plasticity through chronically reduced Ca<sup>+</sup> flux during uncorrelated activity. *Neuron.* 2004; 44:835–849. [PubMed: 15572114]
- Sorra KE, Harris KM. Occurrence and three-dimensional structure of multiple synapses between individual radiatum axons and their target pyramidal cell in hippocampal area CA1. *J Neurosci.* 1993; 13:3736–3748. [PubMed: 8366344]
- Stevens CF, Wang Y. Changes in reliability of synaptic function as a mechanism for plasticity. *Nature.* 1994; 371:704–707. [PubMed: 7935816]
- Sutton MA, Ito HT, Cressy P, Kempf C, Woo JC, et al. Miniature neurotransmission stabilizes synaptic function via tonic suppression of local dendritic protein synthesis. *Cell.* 2006; 125:785–799. [PubMed: 16713568]
- Thiagarajan TC, Lindskog M, Tsien RW. Adaptation to inactivity in hippocampal neurons. *Neuron.* 2005; 47:725–737. [PubMed: 16129401]
- Turrigiano GG, Nelson SB. Hebb and homeostasis in neuronal plasticity. *Curr Opin Neurobiol.* 2000; 10:358–364. [PubMed: 10851171]
- Walmsley B, Edwards FR, Tracey DJ. Nonuniform release probabilities underlie quantal synaptic transmission at a mammalian excitatory central synapse. *J Neurophysiol.* 1988; 60:889–908. [PubMed: 2845016]
- Wierenga CJ, Walsh MF, Turrigiano GG. Temporal regulation of the expression locus of homeostatic plasticity. *J Neurophysiol.* 2006; 96:2127–2133. [PubMed: 16760351]
- Wittner L, Henze DA, Zaborszky L, Buzsaki G. Hippocampal CA3 pyramidal cells selectively innervate aspiny neurons. *Eur J Neurosci.* 2006; 24:1286–1298. [PubMed: 16987216]
- Zakharenko SS, Zablow L, Siegelbaum SA. Visualization of changes in presynaptic function during long-term synaptic plasticity. *Nat Neurosci.* 2001; 4:711–717. [PubMed: 11426227]

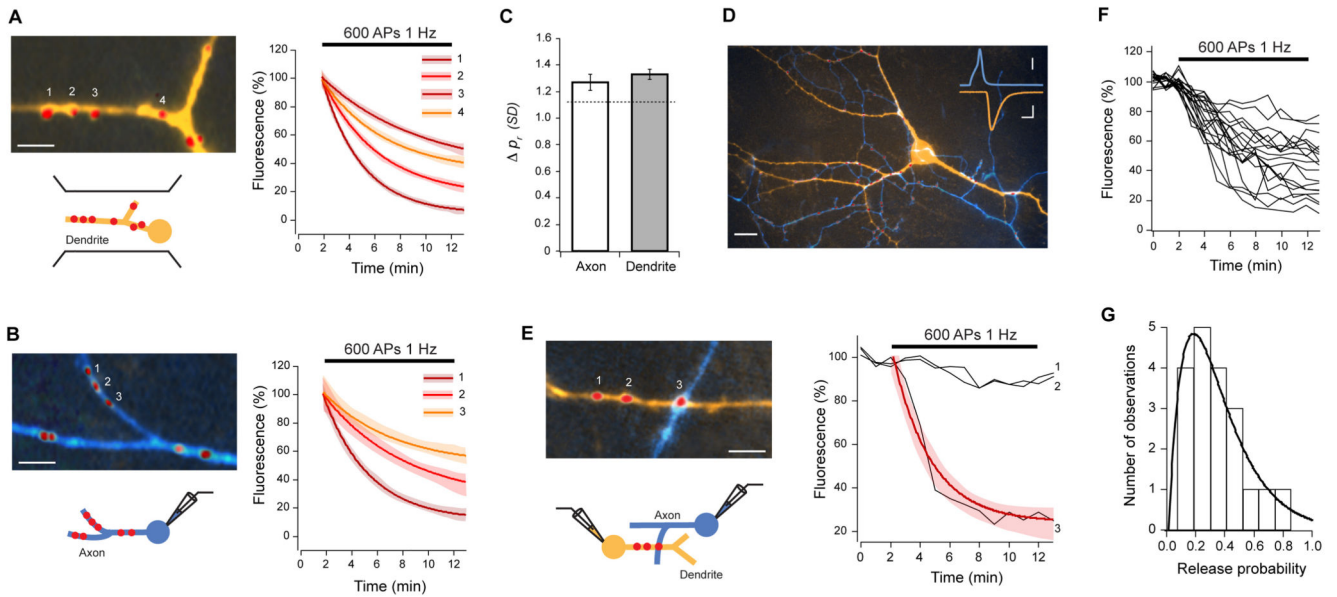


### Figure 1. Variability of release probability.

Release probability was measured by labeling synapses with FM-dye and monitoring destaining rates upon action potential stimulation, delivered by field stimulation (A), or during single (B) and paired (E) whole-cell recordings. (A) Left, dendrite (orange) with FM4-64 labeled synapses (red). Right, destaining curve fits with 95% confidence interval (shaded areas) for the numbered synapses show a wide range of release probabilities for synapses in the same dendritic branch. (B) Left, axon (blue) with several synapses (red), and respective destaining curve fits (right), also show very different  $p_r$ s for synapses along single axons. (C) Summary data of similarity comparisons for all synapses in a branch of dendrite or axon, showing that the mean  $p_r$  difference is not significantly different from the average  $p_r$  difference expected by chance (1.13 SDs, Wilcoxon rank sum test for axon  $P=0.4241$ , dendrite  $P=0.2079$ ). (D) Epifluorescence image of axon (blue) making multiple synaptic contacts (red, FM4-64) with a postsynaptic cell (orange). Inset: representative traces of AP (blue) and evoked EPSC (orange). Scale bars, 15  $\mu\text{m}$ ; inset, 2 ms, 20 mV (top), 100 pA (bottom). (E) Stimulation of the presynaptic cell selectively destains FM4-64 fluorescence from the synapse belonging to the labeled axon (3), and not from those originating from unlabeled axons (1,2). Red line is a single exponential fit. (F, G) Destaining traces from 19 synapses from one connection (F) and corresponding release probability frequency histogram (G). Solid line is gamma function fit ( $\lambda = 5.8$ ,  $n = 3$ ).



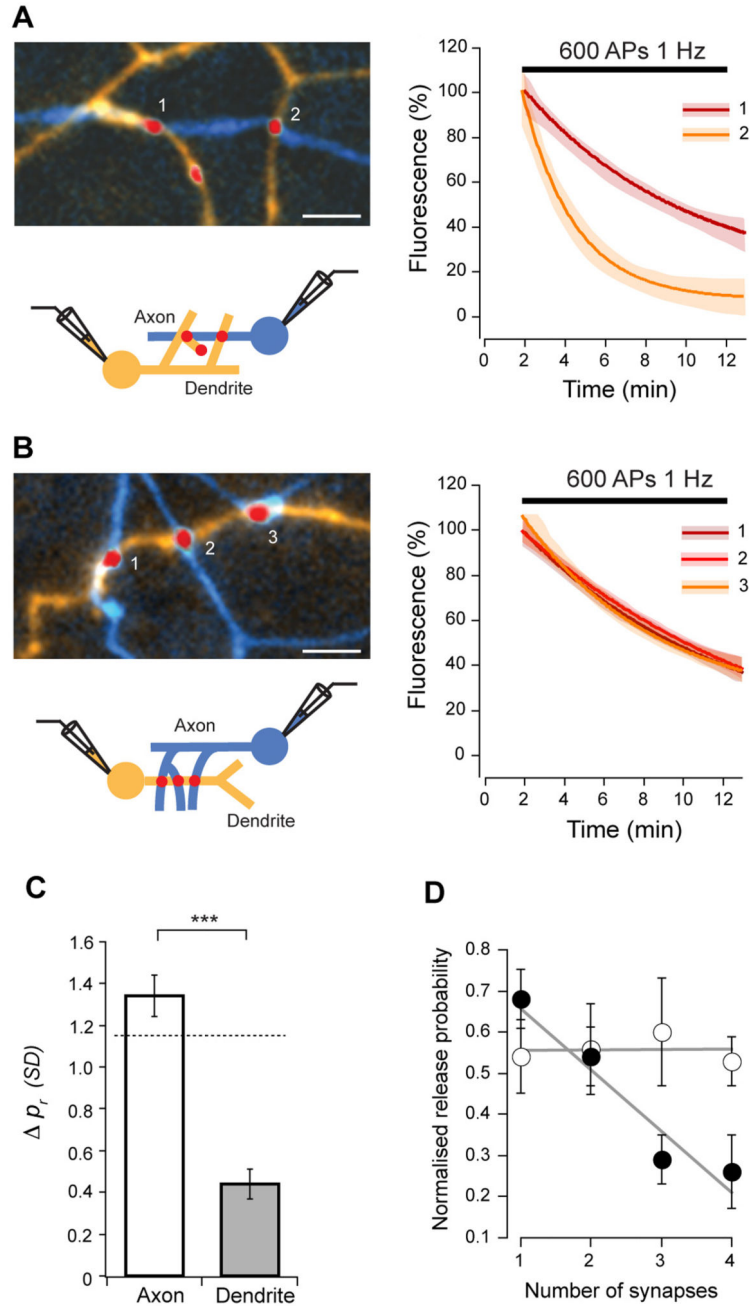


**Figure 2. Release probability is dendritically segregated.**

(A, B) Images (left) and destaining curve fits (right) for synaptic contacts between a cell pair, on different (A) or same dendritic branches (B) of the postsynaptic neuron (axon is blue and dendrite is orange). Release probability of synapses in the same dendritic branch is very similar. (C) Summary of similarity comparisons between synapse pairs. Dashed line indicates expected mean difference due to chance from Monte Carlo simulations (1.15 SDs, Wilcoxon rank sum test for axon  $P=0.1023$ , dendrite  $P<0.0001$ ). Mean intersynaptic distances were not significantly different (axon vs. dendrite,  $P=0.1406$ , axon =  $8.5 \pm 5.3 \mu\text{m}$

(SD), dendrite =  $5.9 \pm 3.0 \mu\text{m}$  (SD)). (D) Normalized release probability plotted against number of synapses in the axonal branch (open circles) and in the dendritic branch (closed circles).  $p_r$  homeostatically adapts to the number of synapses made by the presynaptic cell onto the same dendritic branch. Lines are linear fits to the data. Scale bars,  $5 \mu\text{m}$ . Error bars are  $\pm$  s.e.m.

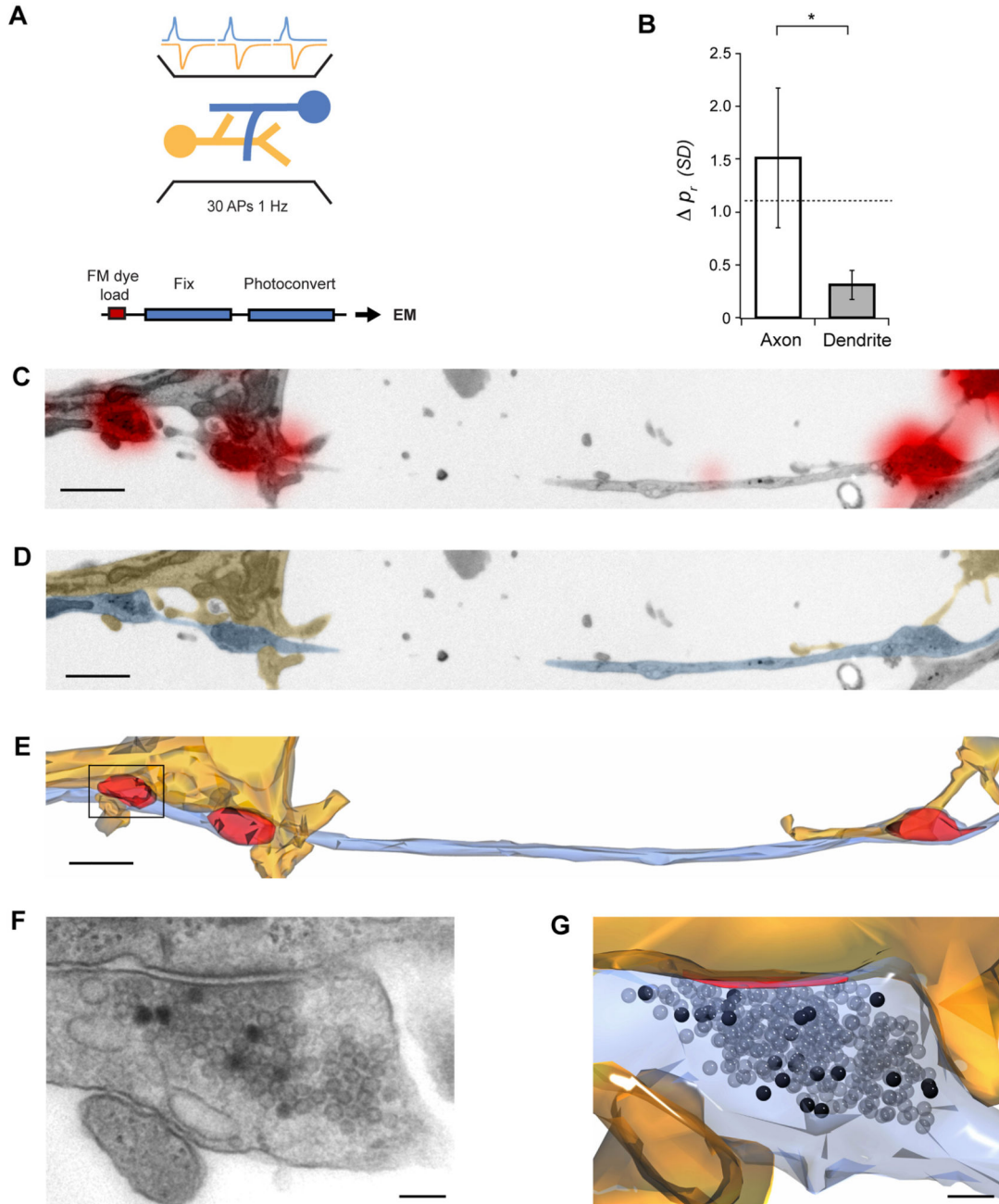


**Figure 3. Ultrastructural analysis of release probability.**

(A) Experimental scheme. FM-dye was loaded into synapses with 30 APs delivered by field stimulation, and samples were photoconverted, serially sectioned, imaged and reconstructed. Release probability was estimated by counting the number of photoconverted vesicles. (B) Summary of similarity comparisons, showing that synapses on the same dendrite have very similar release probabilities (axon vs. dendrite,  $P = 0.0438$ ). Dashed line indicates the expected difference due to chance from Monte Carlo simulations (1.1 SDs, Wilcoxon rank sum test for axon  $P = 0.8750$ , dendrite  $P = 0.0156$ ). (C-E) Representative experiment

showing one axon (blue) making synapses (red) with two different dendrites (orange). (C) Low magnification electron micrograph with FM-dye fluorescence overlaid. (D) Same micrograph as in C with axon and dendrite colored for clarity. (E) 3-D reconstruction with vesicle clusters in red. (F) Higher magnification micrograph of the boxed synapse in E where photoconverted vesicles are clearly seen. (G) 3-D reconstruction of the same synapse with photoconverted vesicles (black) and active zone (red). Scale bar in (C-E), 1  $\mu\text{m}$ , (F, G), 100 nm. Error bars are  $\pm$  s.e.m.

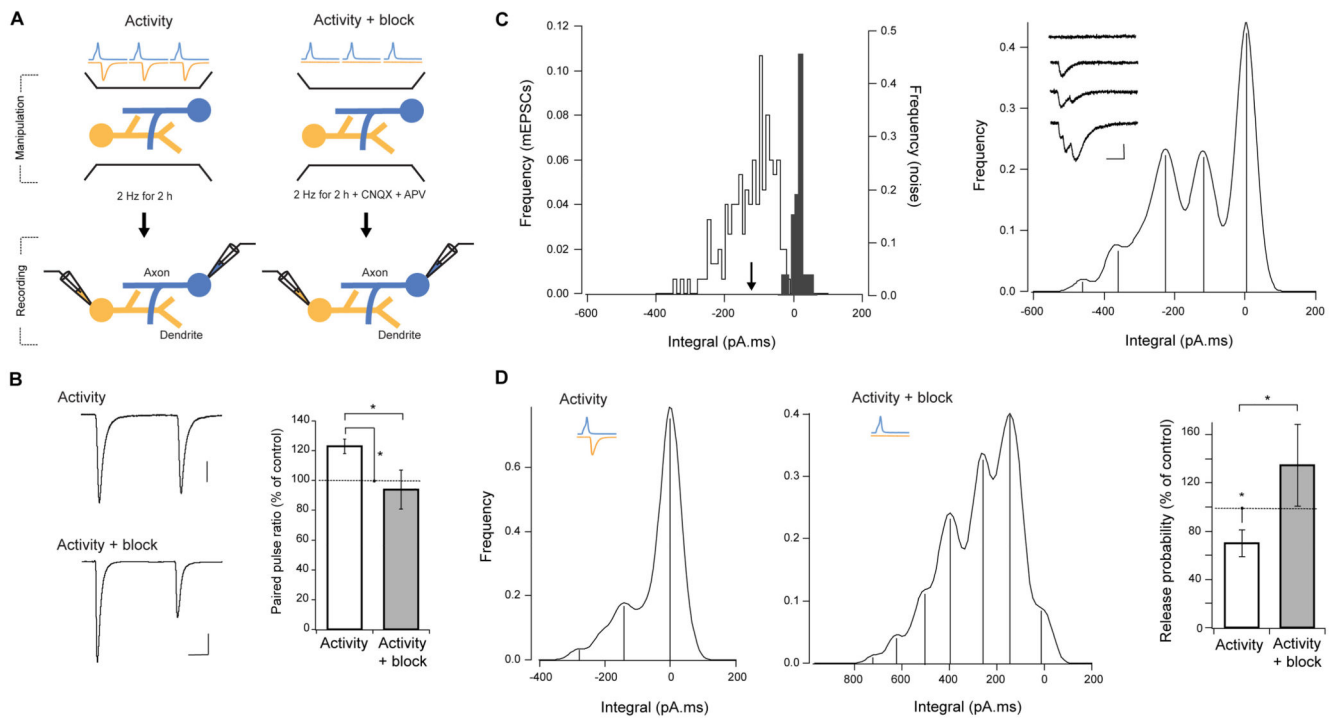


**Figure 4. Release probability is set by dendritic activity.**

(A) Two experimental schemes: activity (left) and activity + block (right). (Left) Activity in the culture was increased by delivering APs with field stimulation for 2 h, and paired whole-cell recordings were used to access the impact of this manipulation on release probability. (Right) For activity + block condition, a similar experimental scheme was used, but excitatory synaptic activity was blocked during stimulation. (B) Example paired-pulse EPSC traces (left, averages of 20) and summary of paired-pulse EPSC amplitude ratio (right), showing an increase of PPR with activity, which is abolished by synaptic blockers. Scale bars, 15 ms, 200 pA top, 100 pA bottom. (C, D) Recordings in 1 mM  $\text{Ca}^{2+}$  / 3 mM  $\text{Mg}^{2+}$ . (C, left) Frequency histogram of mEPSCs integral (white) and baseline noise (gray). Arrowhead indicates the mEPSC integral mean. (C, right) Smoothed histogram of evoked responses integral on the same postsynaptic cell, showing well defined peaks at equally spaced distances. Note that first two peaks correspond to the baseline noise and mEPSC mean in the left panel. Inset shows example traces where different number of quanta have been released. Scale bar, 2 ms, 50 pA. (D) Increasing activity leads to a significant decrease in release probability, which is abolished by blocking excitatory synaptic transmission. Smoothed integral histograms of evoked responses for example connections are shown, after increased activity alone (left), and with synaptic blockers (centre). (D, right) Summary of  $p_r$  changes for all connections.

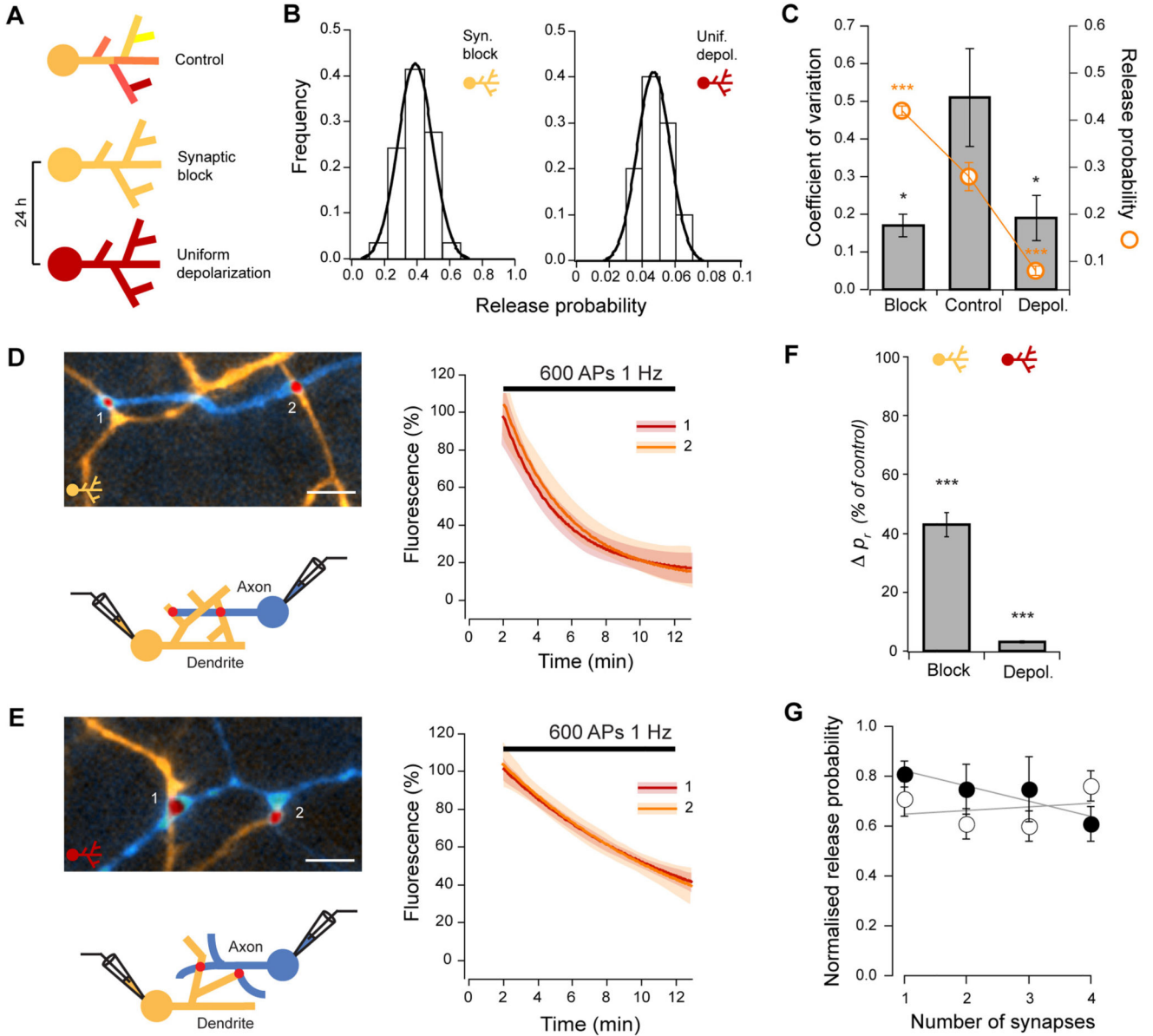


**Figure 5. Variability of release probability results from local adaptations to dendritic activity.** (A) Experimental scheme. Inputs to the dendrite were made uniform pharmacologically by treating cultures for 24 h under ‘synaptic block’ (CNQX, APV, bicuculline) or ‘uniform depolarization’ (CNQX, APV, bicuculline, 20 mM KCl). Release probability was measured by the FM-dye destaining rate in paired recordings, as in Figs. 1 and 2. (B) Frequency histograms for two example connections show opposite changes in  $p_r$  for synaptic block (left) vs. uniform depolarization (right). Lines are Gaussian fits. Note change in the shape of the distribution compared with Fig. 1D. (C) Data summary showing significant decreases in global  $p_r$  CV, and homeostatic changes in  $p_r$ . (D, E), Example connections of synapses on different dendrites (left), and respective fits to FM4-64 destaining curves (right) for synaptic block (D) and uniform depolarization (E). Scale bars, 5  $\mu$ m. (F) Summary of similarity

comparisons for both conditions, show that the mean  $p_r$  difference for synapses on different dendrites is significantly reduced after the activity manipulations. (G) Release probability normalized for each connection plotted against the number of synapses in the dendrite for block (open circles) and uniform depolarization (closed circles). The relationship between  $p_r$  and synapse density is lost (see Fig. 2D). Lines are linear fits to the data.

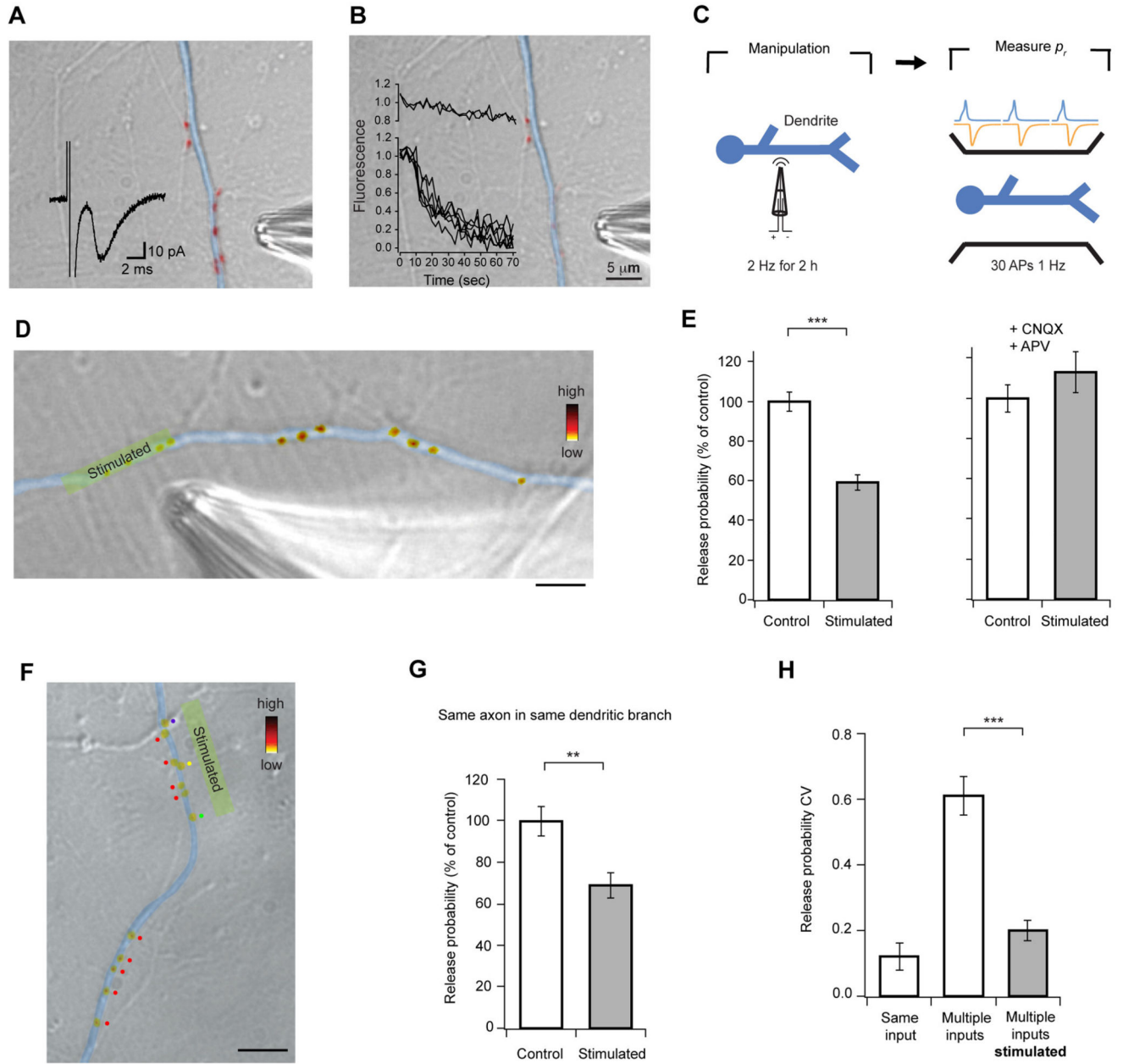


**Figure 6. Local stimulation decreases release probability selectively.**

(A, B) Theta-glass pipette stimulation produces a localized synaptic response. (A) Synapses were labeled with FM-dye (red), and a whole-cell recording established. An EPSC (inset trace) was evoked by positioning the stimulating pipette in front of a group of synapses on the dendrite of the recorded cell (colored in blue for clarity), confirming successful synaptic stimulation. (B) The same synapses were stimulated by 1200 APs at 20 Hz, and FM-dye fluorescence monitored. Inset graph shows that only the group of synapses directly in front of the pipette lost FM-dye fluorescence, indicating high spatial selectivity of the stimulus. (C) Local stimulation was used to increase synaptic activity in a restricted part of a dendritic branch, and  $p_r$  estimated subsequently by loading synapses with FM-dye. (D) Example DIC



image of a dendritic branch with a group of synapses, which were stimulated for 2 h, with superimposed pseudocolored FM4-64 puncta. Fluorescence intensity represents  $p_r$ . Scale bar, 5  $\mu\text{m}$ . (E) Data summary showing that  $p_r$  decreases only in stimulated synapses, and that this effect is abolished by synaptic blockers. (F) Another example image of the same experiment shown in D, where synapses of interest have been categorized according to the axon they belong to (color dots, see Fig. S6 for details on axon tracing procedure). Scale bar, 10  $\mu\text{m}$ . (G) Data summary showing that local stimulation selectively decreases  $p_r$  even if synapses on the dendritic branch belong to the same presynaptic input. (H) Summary data demonstrating that  $p_r$  of synapses from different inputs becomes similar after stimulation. Error bars are  $\pm$  s.e.m.